

Toward Better Medical Diagnosis: Tissue Optical Clearing

Omnia Hamdy^{1,*}, Rania M. Abdelazeem¹

¹Department of Engineering Applications of Laser, National Institute of Laser Enhanced Sciences (NILES), Cairo University, Giza Governorate 12613, Egypt

Abstract

Reaching efficient, safe and painless medical diagnosis procedure is a very valued goal for many research areas. Despite the great advantages of using optical imaging techniques in medical diagnosis including high safety and relative simplicity, it still suffers from relatively low resolution and penetration depth in the multiple scattering mediums such as biological tissues. Therefore, researchers began to devise ways to reduce the scattering properties of the tissue, hence increasing the imaging contrast. Optical clearing concept is introduced to do this job. This technique can reduce tissues scattering properties by using high refractive index chemicals, thus making the tissue transparent by equalizing the refractive index through that medium. In this paper, theory and techniques of optical clearing method are illustrated utilizing its benefits for deep imaging of different body tissues and organs.

Corresponding author: Omnia Hamdy, Department of Engineering Applications of Laser, National Institute of Laser Enhanced Sciences (NILES), Cairo University, Giza Governorate 12613, Egypt. Tel: +20-100-698-3154. Email: omnia@niles.edu.eg

Key words: optical clearing, tissue scattering, medical imaging, diagnosis

Received: Dec 17, 2019

Accepted: Dec 31, 2019

Published: Jan 01, 2020

Editor: Angela Pia Cazzolla, University of Bari, Italy.

Introduction

The relatively low optical penetration as a result of the scattering properties of biological tissues is considered the main limitation of many optical imaging techniques. The principal reason of this multiple scattering characteristics is the difference in the refractive indices between the tissue cell components and its background [1]. The tissue components such as cell nuclei, collagen, elastin fiber, mitochondria, organelles, cytoplasm and plasma membrane of the cell have refractive indices ranging from 1.47 to 1.51, while the surrounding medium has refractive index equals to 1.33, similar to that of water. This causes light diffusion and scattering inside biological tissues [2]. Therefore, a trend has emerged from scientific research towards discovering ways of reducing scattering basically by means of refractive index matching. This research area has been named optical clearing [3]. From the beginning of the 21st century, much more research items related to optical clearing techniques started to show up with a great increasing from 2013 till now [4]. The method started to attract researchers from different areas including physics, chemistry, bioengineering and medicine. Recent studies have been aimed at altering turbid biological tissues in such a way that they become more optically transparent while keeping their internal structure intact using chemical compound with distinct osmotic properties such as glucose and glycerol [5].

After applying optical clearing agents (OCAs), tissue optical scattering parameters "anisotropy and scattering coefficient" have to be calculated to ensure the reduction in the scattering properties of the treated tissue. Determination of tissue optical parameters can be achieved using either integrating sphere measurements [6] or distant detector based configuration [7].

Optical Clearing Techniques

Tissue optical clearing can be achieved using different techniques; physical, chemical, photo-chemical/ photo-thermal and compression. However, choosing the suitable clearing protocol is mostly depending on the size and the physical properties of the analyzed tissue sample [8]. The schematic diagram presented in Figure 1 summarizes the main clearing techniques.

In the physical optical clearing approach, the clearing is achieved by using refractive index matching

solutions in order to reduce the optical inhomogeneity of the tissue sample, these solutions can be either organic or aqueous [4] [9]. The organic optical clearing agents are organic solutions with high refractive index and the clearing process is implemented by two steps: dehydration and clearing. In the dehydration step, the water content of the studied sample is removed commonly using methanol, ethanol, tert-butanol, or tetrahydrofuran, while for the clearing step, methyl, benzyl alcohol/ benzyl benzoate, salicylate, dichloromethane, tertbutanol or dibenzyl ether are widely used [10].

Benzyl Alcohol, Benzyl Benzoate (BAAB) [11], 3D Imaging of Solvent-Cleared Organs (3DISCO) [12] and Polyethylene (PEG)- Associated Solvent System (PEGASOS) [13] are the most common organic solvent-based clearing techniques. Although the organic agents can make the tissue sample transparent in a relatively short time "may be hours", this category suffers from some drawbacks such as high toxicity, tissue shrinkage and endogenous fluorescence quenching [4] [14].

The fact that glycerol has a refractive index about 1.4 makes the use of a solution of glycerol and water (80% of glycerol, $n = 1.44$) suitable for tissue optical clearing. This clarifies the basic idea of using aqueous solutions for tissue clearing [14]. Glycerol based solution is not the only effective approach but also sugar solutions including glucose, fructose and sucrose have been widely used as aqueous clearing agents [15]. This approach is considered relatively safe because it is not toxic and improves the protein fluorescence. However, its clearing efficiency is relatively low compared with the organic based agents [4].

Chemical optical clearing techniques are sometimes termed "tissue transformation" because it depends on removing the lipid contents from the tissue sample in order to reduce the refractive index mismatching through the tissue [16]. Lipid extraction is implemented using electrophoretic tissue clearing (ETC) chamber to apply an electric field [17] or can be achieved passively without ETC [18]. From this base, various techniques have been devised to apply the chemical optical clearing approach such as CLARITY [19], Clear^T[20], SeeDB [21], CUBIC [22] and PACT [23].

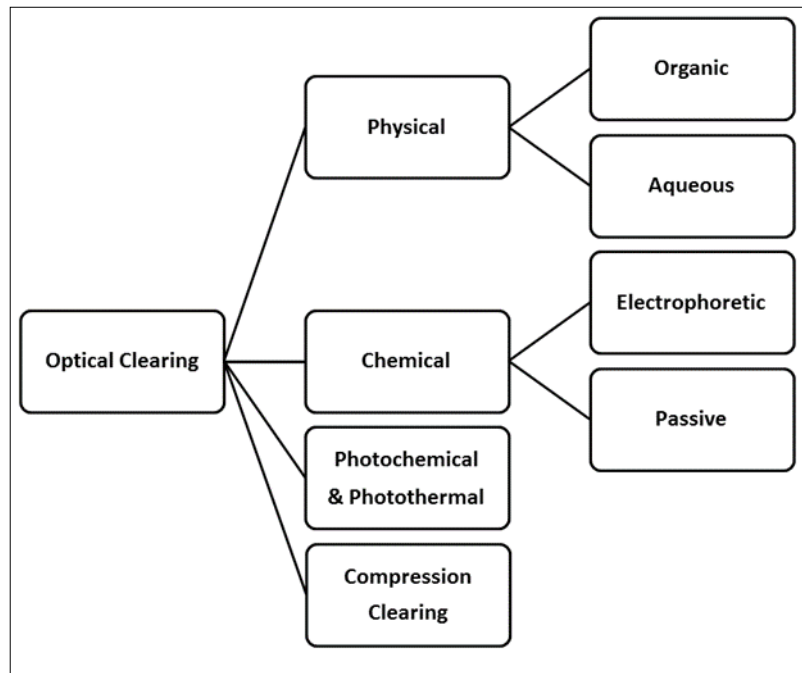


Figure 1. Different clearing techniques

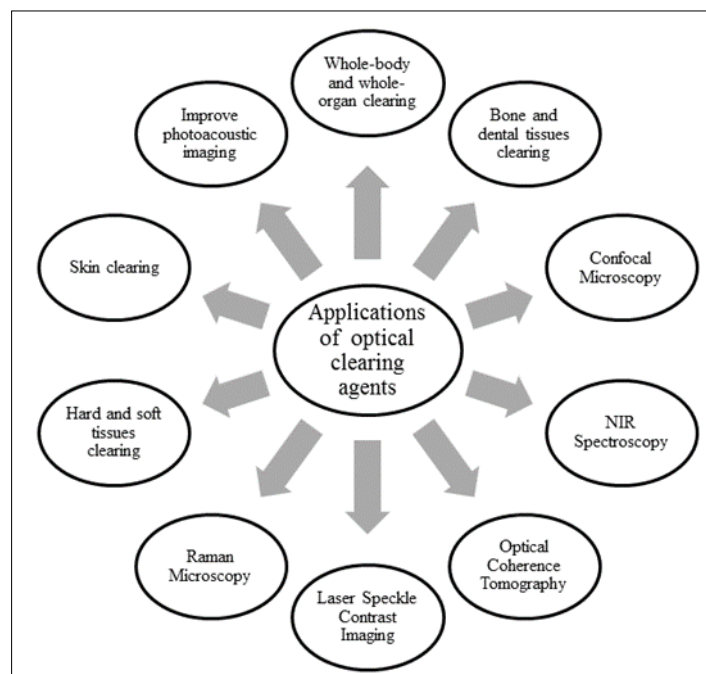


Figure 2. Main applications of optical clearing agents

The optical properties of a biological tissue differ if it is heated; this is the principle of "Photo-thermal & Photo-chemical" optical clearing approach. In such technique, laser radiation is utilized to control the optical scattering properties of the tissue fat [24]. The propagation of light inside biological tissue differs with its morphologic as well as physiological characteristics; therefore, the tissue optical scattering properties can be also changed if the tissue is mechanically compressed. This is the basic idea of the compression clearing methods [25]. Various studies proved that, the induced mechanical force can almost produce the same clearing results as the standard OC steps [26] including increase in optical parameters modification and penetration depth [27].

Selected Medical Applications of Optical Clearing

Optical clearing "OC" methods have been widely utilized to improve medical diagnosis process by enhancing the resolution and the contrast of several medical imaging and spectroscopic systems for both ex-vivo and in-vivo studies [28] as illustrated in Figure 2. Recently, OC techniques has a supportive role in increasing the signal to noise ratio in both Raman and Confocal Microscopy, in addition to improving the visualization of NIR Spectroscopy [29]. Glycerol and glycol based OC were also utilized to improve the speckle contrast of the Laser Speckle Contrast imaging technique [30] and enhancing imaging contrast in different Optical Coherence Tomography (OCT) applications [31].

Many OC approaches have been implemented to investigate their ability to reduce the scattering and increase the light penetration in skin [32]. Anhydrous glycerol was employed to optically clear porcine skin in-vitro. The penetration depth and reduced scattering coefficients were determined at different temperatures showing that, the clearing process become more efficient at higher temperature [33]. Glycerol was also used to clear rat skin in-vivo without any distortion in the collagen fiber, however, this procedure led to shrinkage in the dermis layer due to extracting the water content from the tissue [34].

The use of glycerol coupled with metallic and dielectric nanoparticles (titanium dioxide (TiO₂) and silver nitrate (AgNO₃) with glycerol to enhance OCT images (ex-vivo) for human tooth was assessed by

Vanda S. M. Carneiro et. al. [35]. They utilized the effects of these materials on the sample including cell dehydration effect, the compatibility of refractive indices, and the increase of solubility of collagen. Five molars were gathered showing brownish spots and did not have clear cavitations when they were evaluated by visual inspection. The samples were examined after applying OCAs using OCT (central wavelength of 930 nm, bandwidth of 100 nm, 5 mW maximum power, resolution in water and air is 7 and 5.3 μ m respectively, lateral resolution of 8 μ m and penetration depth of light of 1.6 mm). The evaluation was performed along the occlusal surface with standard scanning procedure by capturing two-dimensional OCT images of the same region of representative sample. The OCT image without OCAs was compared to another series of images that covered with glycerol only, glycerol with AgNP, and glycerol with TiO₂ NP (TiO₂ had two concentrations of 0.01 and 0.1%). The results revealed that without applying OCAs, the lesion was not clearly imaged. Moreover, after applying OCAs the image was enhanced due to high penetration of the light as well as sulcus region was better recognized. Furthermore, glycerol with AgNP showed better enhancement than glycerol with TiO₂ NP image.

Optical Clearing was also utilized to improve the visibility of OCT images for tooth roots to achieve better diagnosis of defects or lesion in tooth roots by reducing internal light scattering at the root and increasing the penetration depth [36]. Twenty teeth were gathered and sterilized by gamma radiation. The suspected lesions were clearly seen by its color on the tooth surface including root surface and caries. Consequently, each tooth was submerged in three different solutions (Water, Glycerol (G) and Propylene Glycerol (PG) with refractive indices (n) of 1.3, 1.45, 1.43 and viscosity of 0.89 cP, 1194 cP, 46 cP respectively) before each scan. They used Dentin of refractive index 1.55. Clearing agent's viscosity was a critical factor, the penetration depth of both agent and light decreased at higher viscosity and also the lesion contrast decreased. For Root Lesion Analysis, OCT images were captured in the series wet, dry, PG, wet, dry, G to prevent the interference that might result from the application of different agents. Each sample was washed with water after each agent. a-scans were chosen from b-scan that had surface root

Freely Available Online

lesions of high reflectivity, profile identification and reflectivity integration were calculated using Igor Pro software. The demineralized areas showed higher reflectivity and attenuation that could be discriminated from sound enamel and dentin. The chosen a-scans in lesion areas were normalized and fitted to give a relation between normalized intensity and depth. Their results showed that the intensity decreased with depth in the OCT images. Tactile examination was made on the lesions after all imaging, because it would damage the lesions. Tactile results were evenly soft (considered active), three were leathery and six were hard. Visual examination of the twenty lesions indicated that, five were black, nine were light colored and six were brown. The texture was identified as smooth for six lesions and rough for fourteen lesions. Fifteen of the lesions had a matte appearance while the other five appeared smooth. They measured three values to show the optical penetration of light into the tooth, depth weighted reflectivity, Optical penetration depth and Mean, standard deviation for attenuation coefficient. The optical penetration depth was significantly higher for PG and G than wet and dry. For Subsurface Root Analysis, the relative intensity of the root canal structure was calculated to clarify the influence of the agents on the visibility of structures under the surface. The integrated reflectivity, lesion depth, and maximum intensity were recorded for each specific position. The ratio of the root canal to surface intensity that characterized the visibility of the root canal wall and the integrated reflectivity were increased in case of G and PG. For Lesion Shrinkage Analysis, Avizo software was used to analyze the volumetric OCT images for both wet and dry conditions and to identify volumetric changes and then calculate their area using matlab. For comparison, the shrinkage at a center of the lesion was also calculated. Shrinkage was significant because it had the potential to be used to assess the activity of root lesions. Lesions with high shrinkage were more severe and vice versa. The results showed that optical clearing with OCT could be used to measure the shrinkage of natural root caries lesions in vitro. They showed that 5 lesions and demineralized dentin tended to shrink when they were dried. For Statistical Analysis, Prism from Graphpad Software was used to measure variance for comparison between before, after drying and with applied clearing agents. A paired t-test was used for measurement of shrinkage of

root lesions. Their results showed that the performance of G was slightly better than PG and it was well suited for use in dental imaging due to its availability in market. Optical penetration depth increased by almost a factor of two over wet lesions and by a factor of greater than 5 over the dry lesion if G was utilized [36].

The effect of OC using different concentrations of glucose solution on porcine epithelial tissue samples was inspected [37]. The ear sections were cut into squares of area $1 \times 1 \text{ cm}^2$ and stored in saline solution to prevent dehydration. A gold-plated mirror was imaged below the tissue and clearing percentage was measured from the mirror by observing the change in reflected light intensity over time. As the OCA diffuses through the tissue, it replaces water through osmotic forces which in turn matched the intracellular and extracellular fluids indices of refraction as well as make the tissue more optically homogeneous. Other changes were decreased scattering properties of the tissue resulted from the dissociation of collagen fibers and dehydration of the tissue. They used swept-source OCT system that was implemented utilizing broadband swept-source laser (wavelength of $1325 \pm 50 \text{ nm}$, axial resolution in air of $8 \mu\text{m}$, sweeping frequency of 16 KHz and average power of 10 mW). The penetration depth and the transverse resolution for the used system were 3 mm (in air) and $15 \mu\text{m}$, respectively. A MATLAB code was used to calculate the reflected light intensity from the mirror surface over time that detected the maximum intensity within a specified depth region in an a-scan. They showed that the OCT could quantify and monitor the effects of optical clearing continuously on the skin of porcine. The clearing percentage was monitored as a function of intensity changes of reflected light from the mirror over time. The results indicated that as the concentration of glucose solution increased, the high optical clearing could be obtained. Also, the thickness of tissue changed by 25%, 6% and 4% with using 50%, 30% and 10% of glucose concentrations, respectively. For their future studies, they intend to determine the proper concentration of OCA that could significantly improve the contrast without damaging other tissues [37].

Liu *et. al.* [38] utilized the integration of OCA with acoustic resolution photoacoustic microscopy (AR-PAM) to enhance the imaging of subcutaneous blood vessels of dorsal skin. Their system was

Table 1. Main literature findings in tissue optical clearing

Tissue	Clearing method	Clearing agent / protocol	Observation technique	Clearing capability	Reference
Gastrointestinal Tissues	In-vitro	Propylene Glycol	Optical Coherence Tomography	More detailed microstructures	Wang et. al. [31]
Squamous Epithelial Tissue	In-vivo	dimethyl sulfoxide (DMSO), Glycerol	Reflectance spectrum	DMSO is more efficient than Glycerol	Millon et al. [43].
Human eye sclera	In-vitro	Glucose	Spectrophotometer	Significantly decrease in scattering	Bashkatov et al. [39]
Rat skin	In-vivo	Glycerol	Reflectance spectrum, optical and electron microscopy.	Decrease in reflectance, thickness of dermis and the diameter of the collagen fibers	Wen et al. [34]
Porcine skin	In-vitro	Glucose	Swept-Source Optical coherence tomography	The highest optical clearing effect at 50% glucose	Sudheendra n et al. [37]
Porcine skin	In-vitro	Anhydrous Glycerol	Spectrometry combined with integrating sphere	Decrease scattering by 76.6%, and increase penetration depth by 84.1% at 45°C	Deng et al. [33]
Rat dorsal skin	Ex-vivo	DMSO Glycerol Glucose	Photoacoustic detection	Improve in detecting deep-sealed blood vessels and image quality of shallow vessels	Liu et. al. [38]
Musculoskeletal tissues	In-vitro	Fructose	Stereo dissecting microscope	Enabled in situ patterns of osteocyte processes and the lacunar-canalicular system deep within mineralized cortical bone	Clave et. al. [41]
Brain tumor tissues	Ex-vivo	CLARITY hydrogel. methanol iDISCO	3D microscopy	More detailed 3D visualization	Lagerweij et. al. [44]
Human dura mater	In-vitro	Glucose	Multichannel spectrometer	Different clearing efficiency at different glucose concentrations	Genina et. al. [45]
Tooth hard tissues	In-vitro	glycerol associated to titanium dioxide and silver nitrate nanoparticles	Optical coherence tomography	Better distinction of healthy and demineralized hard tissues in occlusal surfaces	Carneiro et. al. [35]
Tooth root	In-vitro	Glycerol propylene glycol	Optical coherence tomography	Improve diagnosis of root caries and other defects on root surfaces.	Yang et. al. [36]

constructed by an optical condenser and a conical lens to provide the dark-field illumination, and an ultrasonic transducer to measure the induced ultrasonic waves. Furthermore, a water tank was used to integrate the ultrasonic wave between the transducer and sample. The dorsal skin was prepared not including the subcutaneous fat and the stratum corneum, and then it was submerged in OCA. They used fibers of carbon to assess the spatial resolution of the AR-PAM. Moreover, the photoacoustic amplitude was measured by black tape and calibrated by a laser diode. The immersed sample in PEG-400 began to decrease the photoacoustic signal after more than thirty minutes due to breakdown of fibers and dehydration which in turn caused decreased resolution. In case of oleic acid, glycerol and glucose, the photoacoustic signal decreased. For in-vivo experiments, they selected PEG-400 with thiazone, DMSO and glycerol. They imaged the samples before applying OCAs to gather control images and after fifteen minutes from applying OCAs. The results revealed that in case of PEG-400 with thiazone, the resolution was enhanced greatly without changing the vascular diameter and the photoacoustic amplitude was increased by two times. So, it was suitable for imaging deep blood vessels. By using glycerol, the optical clearing was decreased but the photoacoustic signal amplitude was increased by half, dehydration was not noticed, so it was appropriate for imaging shallow vessels. For DMSO, the optical clearing was poor, the observed amplitude of the vessel was 30% of its original value and the vascular diameter was increased. In conclusion, the improvement in the amplitude of photoacoustic signal was caused by enhanced optical transmittance with dehydration. Moreover, the immersion time should be carefully controlled to prevent weakening in photoacoustic signal.

In another study, the optical absorption and scattering properties of human eye sclera were studied after treated with 40% glucose solution over a wide range of wavelength (400-1800 nm) in-vitro showing sufficient drop in the reduced scattering coefficient of the studied samples [39]. In practice, OC technology has been successfully applied for clearing both soft and hard tissues as well [40] [41]. Moreover, it has been utilized in bone research to facilitate 3D imaging with no sectioning of bone [42]. Table 1 gathers the main literature findings in different practices and applications of tissue optical clearing.

Conclusion

With promising achievements, the use of tissue optical clearing has proven remarkable success in many medical diagnosis procedures. However, more investigations are still required to achieve the best possible results ensuring safety use and minimum biological harm.

References

1. D. S. Richardson and J. W. Lichtman, "Clarifying Tissue Clearing," *Cell*, vol. 162, pp. 246–257, 2015.
2. E. A. Genina, A. N. Bashkatov, Y. P. Sinichkin, I. Y. Yanina, and V. V. Tuchin, "Optical clearing of biological tissues: prospects of application in medical diagnostics and phototherapy," *J Biomed. Photonics Eng*, vol. 1, no. 1, pp. 23–58, 2015.
3. E. A. Genina, A. N. Bashkatov, and V. V. Tuchin, "Tissue optical immersion clearing," *Expert Rev. Med. Devices*, vol. 7, no. 6, pp. 825–842, 2010.
4. I. R. C. Ostantini, R. I. C. Icchi, L. U. S. Ilvestri, F. R. V Anzi, and F. R. S. A. P. Avone, "In-vivo and ex-vivo optical clearing methods for biological tissues: review," *Biomed. Opt. Express*, vol. 10, no. 10, pp. 5251–5267, 2019.
5. E. A. Genina, A. N. Bashkatov, K. V. Larin, and V. V. Tuchin, "Light Tissue Interaction at Optical Clearing," in *Laser Imaging and Manipulation in Cell Biology*, 2010, pp. 115–163.
6. O. Hamdy, M. Fathy, T. A. Al-Saeed, J. El-Azab, and N. H. Solouma, "Estimation of optical parameters and fluence rate distribution in biological tissues via a single integrating sphere optical setup," *Optik (Stuttg)*, vol. 140, 2017.
7. O. Hamdy, J. El-Azab, T. A. Al-Saeed, M. F. Hassan, and N. H. Solouma, "A method for medical diagnosis based on optical fluence rate distribution at tissue surface," *Materials (Basel)*, vol. 10, no. 9, 2017.
8. J. H. Kim *et al.*, "Optimizing tissue-clearing conditions based on analysis of the critical factors affecting tissue-clearing procedures," *Sci. Rep.*, vol. 8, no. 12815, pp. 1–11, 2018.
9. D. Zhu, K. V Larin, Q. Luo, and V. V Tuchin, "Recent progress in tissue optical clearing," *Laser Photonics Rev.*, vol. 757, no. 5, pp. 732–757, 2013.
10. A. Azaripour, T. Lagerweij, C. Scharfbillig, E.

Freely Available Online

- Jadczak, B. Willershausen, and C. J. F. Van Noorden, "A survey of clearing techniques for 3D imaging of tissues with special reference to connective tissue," *Prog. Histochem. Cytochem.*, vol. 51, no. 2, pp. 9–23, 2016.
11. D. S. Foster *et al.*, "A Clearing Technique to Enhance Endogenous Fluorophores in Skin and Soft Tissue," *Sci. Rep.*, vol. 9, no. 15791, pp. 1–8, 2019.
 12. C. Pan *et al.*, "Shrinkage-mediated imaging of entire organs and organisms using uDISCO," *Nat. Methods*, vol. 13, no. 10, p. 859, 2016.
 13. D. Jing *et al.*, "Tissue clearing of both hard and soft tissue organs with the PEGASOS method," *Cell Res.*, vol. 28, pp. 803–818, 2018.
 14. E. C. Costa and D. N. Silva, "Optical clearing methods: An overview of the techniques used for the imaging of 3D spheroids," *Biotechnol. Bioeng.*, vol. 116, no. 10, pp. 2742–2763, 2019.
 15. V. G, C. EK, B. JK, R. HG, and W. AJ, "Use of an agent to reduce scattering in skin.," *Lasers Surg Med*, vol. 24, no. 2, pp. 133–141, 1999.
 16. H. A. O. Du, P. Hou, W. Zhang, and Q. Li, "Advances in CLARITY - based tissue clearing and imaging (Review)," *Exp. Ther. Med.*, vol. 16, pp. 1567–1576, 2018.
 17. K. Chung, J. Wallace, S.-Y. Kim, S. K. A. S. Andalman, and T. J. Davidson, "Structural and molecular interrogation of intact biological systems," *Nature*, vol. 497, no. 7449, pp. 332–337, 2014.
 18. B. Yang, J. B. Treweek, R. P. Kulkarni, B. E. Deverman, C. Chen, and E. Lubeck, "Single-Cell Phenotyping within Transparent Intact Tissue through Whole-Body Clearing," *Cell*, vol. 158, no. 4, pp. 945–958, 2014.
 19. H. Du, P. Hou, L. Wang, Z. Wang, and Q. Li, "Modified CLARITY Achieving Faster and Better Intact Mouse Brain Clearing and Immunostaining," *Sci. Rep.*, vol. 9, no. 10571, pp. 1–11, 2019.
 20. T. Kuwajima, A. A. Sitko, P. Bhansali, C. Jurgens, W. Guido, and C. Mason, "Clear T: a detergent- and solvent-free clearing method for neuronal and non-neuronal tissue," *Development*, vol. 140, no. 6, pp. 1364–1368, 2013.
 21. M.-T. Ke, S. Fujimoto, and T. Imai, "Optical Clearing Using SeeDB," *Bio-protocol*, vol. 4, no. 3, p. e1042, 2014.
 22. E. A. Susaki, K. Tainaka, D. Perrin, H. Yukinaga, A. Kuno, and H. R. Ueda, "Advanced CUBIC protocols for whole-brain and whole-body clearing and imaging," *Nat. Protoc.*, vol. 10, no. 11, pp. 1709–1727, 2015.
 23. P. H. Neckel, U. Mattheus, B. Hirt, L. Just, and A. F. Mack, "Large-scale tissue clearing (PACT): Technical evaluation and new perspectives in and ultrastructure," *Sci. Rep.*, vol. 6, no. 34331, pp. 1–13, 2016.
 24. V. V Tuchin, I. Y. Yanina, and G. V Simonenko, "Destructive fat tissue engineering using photodynamic and selective Destructive fat tissue engineering using photodynamic and selective photothermal effects," in *Proc. of SPIE*, 2009, no. 7179, pp. 71790C-1–11.
 25. E. K. Chan, B. Sorg, D. Protsenko, M. O. Neil, M. Motamedi, and A. J. Welch, "Effects of Compression on Soft Tissue Optical Properties," *IEEE J. Sel. Top. Quantum Electron.*, vol. 2, no. 4, pp. 943–950, 1996.
 26. C. W. Drew and C. G. Rylander, "Mechanical compression for dehydration and optical clearing of skin," in *Proceeding of the ASME*, 2008, pp. 2–3.
 27. C. G. Rylander, T. E. Milner, S. Baranov, and J. S. Nelson, "Mechanical Tissue Optical Clearing Devices: Enhancement of Light Penetration in Ex-Vivo Porcine Skin and Adipose Tissue Christopher," *Lasers Surg Med.*, vol. 40, no. 10, pp. 688–694, 2008.
 28. M. Inyushin, D. Meshalkina, L. Zueva, and A. Zayas-santiago, "Tissue Transparency In Vivo," *Molecules*, vol. 24, no. 2388, pp. 1–13, 2019.
 29. A. Y. Sdobnov, M. E. Darvin, E. A. Genina, A. N. Bashkatov, J. Lademann, and V. V Tuchin, "Recent progress in tissue optical clearing for spectroscopic application," *Spectrochim. Acta Part A Mol. Biomol. Spectrosc.*, vol. 197, pp. 216–229, 2018.
 30. D. Zhu and J. Wang, "Imaging dermal blood flow through the intact rat skin with an optical clearing method," *J. Biomed. Opt.*, vol. 15, no. 2, pp. 1–7, 2010.

31. R. K. Wang and J. B. Elder, "Propylene Glycol As a Contrasting Agent for Optical Coherence Tomography to Image Gastrointestinal Tissues," *Lasers Surg. Med.*, vol. 30, pp. 201–208, 2002.
32. A. Y. Sdobnov, J. Lademann, M. E. Darvin, and V. V. Tuchin, "Methods for Optical Skin Clearing in Molecular Optical Imaging in Dermatology," *Biochem.*, vol. 84, pp. 144–158, 2019.
33. Z. Deng, C. Liu, W. Tao, and D. Zhu, "Improvement of skin optical clearing efficacy by topical treatment of glycerol at different temperatures Improvement of skin optical clearing efficacy by topical treatment of glycerol at different temperatures," *J. Phys. Conf. Ser.*, vol. 277, no. 012007, pp. 1–8, 2011.
34. X. Wen, Z. Mao, Z. Han, V. V. Tuchin, and D. Zhu, "In vivo skin optical clearing by glycerol solutions: mechanism," *J. Biophoton.*, vol. 3, no. 1–2, pp. 44–52, 2010.
35. V. S. M. Carneiro *et al.*, "Optical Clearing Agents Associated with Nanoparticles for Scanning Dental Structures with Optical Coherence Tomography," in *CLEO*, 2017, pp. 3–4.
36. V. B. Yang, D. A. Curtis, D. Fried, and A. S. Preparation, "Use of Optical Clearing Agents for Imaging Root Surfaces With Optical Coherence Tomography," *IEEE J. Sel. Top. Quantum Electron.*, vol. 25, no. 1, pp. 1–7, 2019.
37. N. Sudheendran, M. Mohamed, M. G. Ghosn, V. V. Tuchin, and K. V. Larin, "Assessment Of Tissue Optical Clearing As A Function Of Glucose Concentration Using Optical Coherence Tomography," *J Innov Opt Heal. Sci.*, vol. 3, no. 3, pp. 169–176, 2011.
38. Y. Liu, X. Yang, D. Zhu, R. Shi, and Q. Luo, "Optical clearing agents improve photoacoustic imaging in the optical diffusive regime," *Opt. Lett.*, vol. 38, no. 20, pp. 4236–4239, 2013.
39. A. N. Bashkatov *et al.*, "Optical clearing of human eye sclera under the action of glucose solution," *Proc. SPIE*, vol. 6535, no. 653515, pp. 1–8, 2007.
40. E. A. Susaki and H. R. Ueda, "Whole-body and Whole-Organ Clearing and Imaging Techniques with Single-Cell Resolution: Toward Organism-Level Systems Biology in Mammals," *Cell Chem. Biol.*, vol. 23, no. 1, pp. 137–157, 2016.
41. S. Calve, A. Ready, C. Huppenbauer, and R. Main, "Optical Clearing in Dense Connective Tissues to Visualize Cellular Connectivity In Situ," *PLoS One*, pp. 1–14, 2015.
42. D. Jing *et al.*, "Tissue Clearing and Its Application to Bone and Dental Tissues," *J. Dent. Res.*, vol. 00, no. 0, pp. 1–11, 2019.
43. S. R. Millon, K. M. Roldan-perez, K. M. Ricking, G. M. Palmer, and N. Ramanujam, "Effect of Optical Clearing Agents on the In Vivo Optical Properties of Squamous Epithelial Tissue," *Lasers Surg. Med.*, vol. 38, pp. 920–927, 2006.
44. T. Lagerweij, S. A. Dusoswa, A. Negrean, J. P. M. Yvette, and V. K. Pieter, "Optical clearing and fluorescence deep-tissue imaging for 3D quantitative analysis of the brain tumor microenvironment," *Angiogenes.*, vol. 20, pp. 533–546, 2017.
45. E. A. Genina, A. N. Bashkatov, and V. V. Tuchin, "Optical clearing of human dura mater by glucose solutions," *J Biomed. Photonics Eng*, vol. 3, no. 1, pp. 010309-1–9, 2017.